Pergamon

Corrosion Science, Vol. 38, No. 6, pp. 889–907, 1996

0010–938X/96 $15.00 + 0.00

PII: S0010–938X(96)00175–1

THE EFFECT OF LEAD IMPURITY ON THE DC-ETCHING BEHAVIOUR OF ALUMINUM FOIL FOR ELECTROLYTIC CAPACITOR USAGE

W. LIN,*† G. C. TU,† C. F. LIN‡ and Y. M. PENG‡

†Institute of Materials Science and Engineering, National Chiao Tung University, Hsinchu Taiwan, R. O. C.
‡Materials Research Laboratories, Industrial Technology Research Institute, Hsinchu Taiwan, R. O. C.

Abstract—The effects of lead impurity on the etched morphology of high purity aluminum foils for electrolytic capacitor applications were investigated in this work. The lead impurity was either present in as-received aluminum foils or deposited purposely on the foil surface through an immersion–reduction reaction. The amount and distribution of deposited lead varies with the lead content in as-received foil. The as-received foil with higher lead content gave a higher concentration and a more uniform distribution of deposited lead. Uniformly distributed vertical tunnel etchings were obtained when high lead foil, formed by immersion as-received high lead foil in $Pb(NO_3)_2$ solution, was subject to DC-etching. For the as-received lower lead foils, the deposited lead was concentrated in rolling lines which resulted in surface etching along rolling lines. Both the surfacial and cross-sectional etching morphologies are presented in this study, together with the etching mechanism discussed.

INTRODUCTION

The capacitance of electrolytic capacitors depends theoretically on the effective surface area of aluminum foil (electrode), the thickness of aluminum oxide film and the dielectric constant of the film. It is well-known that an electrochemical etching process is an effective technique to increase the surface area of aluminum electrode. For the capacitor, size minimization and high voltage applications, vertical tunnel-type etching, rather than surface etching, is demanded.

There are many factors which influence tunnel etching. The properties of raw foils is one of the important factors. The well discussed properties of raw foil which influence the electrochemical etching process are grain size,[1] cubicity[2–4] and impurities or pre-existing flaws of the foil.[5–10] In general, the grain size of aluminum foils for high voltage applications is relatively large, *ca.* $50 \sim 200\ \mu m$. High cubic texture fraction (cubicity) is necessary for tunnel type etching because it has been shown that tunnels are formed preferentially along $< 100 >$ directions in hydrochloric acid.

The effect of impurity elements in aluminum foil, such as Fe, Cu, Si, Mg, Zn, etc. on tunnel etching has also been well discussed. Arai[11] indicated that impurity elements, such as B and Bi in aluminum foil with content as little as ppm level would prompt surface etching, i.e. inhibit tunnel formation, and result in decreased capacitance.

Many researchers[12,13] have indicated that the distribution of surface impurities could be even more important than impurity content. Some earlier work[14] focused on introducing

*To whom all correspondence should be addressed.
Manuscript received 26 June 1995: in amended form 17 October 1995

trace elements, such as Fe and Cu, to increase initial etching sites and to enhance etchability. The problem with introducing these elements is that the leakage current of their oxide film may increase significantly. Recently, an impurity of In[15] was added to aluminum foil, aimed at improving the distribution of etching sites and to enhance tunnel growth.

In the present study on etching of commercialized high purity aluminum foils for electrolytic capacitors, the origins of raw foils were found to influence the etching behaviour tremendously.[16] Under the same etching conditions, some foils produce uniformly distributed vertical tunnels, while others undergo surfacial attacking along rolling lines. From the results of SIMS measurements, it was found that two different origins of aluminum foils, namely Foil A and Foil B, have obviously different peak intensities for element Pb. The etching behaviour of the two foils was also quite different. Since Pb and Al are both fcc crystals with quite different atomic sizes and emf values, it is interesting to study in detail the effect of lead impurity on the etching behavior of commercialized aluminum foil in the present work.

EXPERIMENTAL METHOD

Raw aluminum foils

The raw foils (Foil A and Foil B) used in this work were high purity (99.99%) commercialized aluminum foils, from two suppliers, for high voltage applications. The chemical compositions of the foils were determined by ICP-AES technique, and are shown in Table 1. The cubic texture fraction (cubicity) were determined with X-ray diffractometer (Siemens-D5000) and the grain size of the foils were determined using image analyzer (Quantimet 520, Cambridge) after electro-polishing the foils. The experiment flowchart is shown in Fig. 1.

The depth profile of lead

Secondary ion mass spectrometry (SIMS, CMECA-IMS4F) was used to obtain the depth profiles of lead in the foils. The ion source is O_2^+ and the working current is 400 nA. The spot size is about 5 μm such that Pb content in the rolling line can be characterized. The locations of the foils examined were rolling line area and area in between rolling lines.

Pretreatment and DC-etching

Samples with the dimensions of 2 × 7 cm were degreased in 1 N NaOH at 60°C for 60 s. After rinsing thoroughly with deionized water, the samples were immersed in 50% HNO_3 at 90°C for 30 s. Then the samples were rinsed with deionized water before being transferred to etching cell. For some experiments 0.1 N $Pb(NO_3)_2$, instead of 50% HNO_3, was used to introduce Pb on to the foil surface intentionally.

Table 1. Chemical composition of the sample (wt ppm)

	Sample										
Element	Fe	Si	Cu	Mg	Zn	Mn	Cr	Ni	Ti	Pb	In
A	10.3	8.9	32.9	0.97	0.97	1.8	<1	<2	<1	<2	<30
B	8.9	8.5	27.5	1.20	5.0	1.9	<1	<2	<1	<2	<30

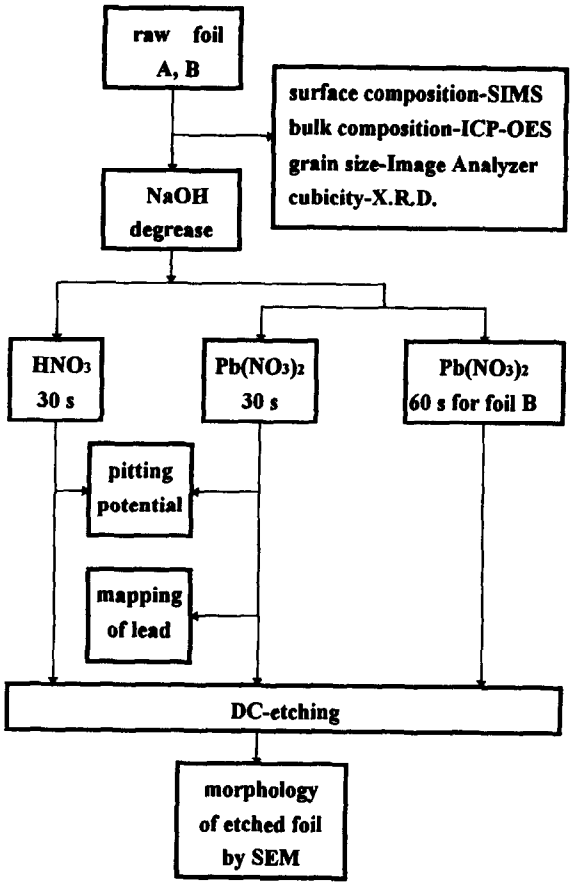

Fig. 1. Flowchart of the experimental procedure.

After pretreatments, samples were mounted on a sample holder with an area of 3 cm^2 exposed to the etching solution. The electrolyte used was 1 N HCl. All solutions used in this work were prepared from reagent grade chemicals and deionized water. A high purity (99.95%), high density graphite was used as counter electrode. A reference electrode (Ag/AgCl/3M KCl) was placed in a fixed position behind the sample holder. All potentials reported in this work are referred to this reference electrode.

Direct current (DC) etching was carried out immediately after placing the sample holder into the electrolyte. A constant current density of 200 mA/cm^2 was applied for 1 and 20 s at 70°C. A potentiostat/galvanostat (Princeton Applied Research, PAR273), interfaced to a personal computer, was used to supply constant current as well as to measure pitting potential.

Pitting potentials of specimens after different pretreatments were measured, in 1 N HCl at 70°C, through cyclic voltammetry technique with a scan rate of 20 mV/min.

Etched morphology observation

After electrochemical etching, the samples were rinsed with deionized water and dried in ambient conditions. For surface morphology studies, the samples were sputter-coated with gold before examining in a scanning electron microscope (SEM, Hitachi-2500). For

sectional observation, which would shed light on tunnel development, the etched samples were anodized, mounted vertically in epoxy resin, mechanically polished, chemically dissolved, sputter-coated with gold and examined under SEM. Details of the above procedure are given elsewhere.[17]

Mapping of lead

Both raw Foil A and Foil B were degreased with NaOH for 60 s, rinsed in deionized water, immersed in 0.1 N $Pb(NO_3)_2$ for 30 s and finally cleaned with deionized water.

Since the atomic weight of lead is much more than that of aluminum, the backscattering electron image (BEI) mode was selected to perform mapping of deposited lead on the foil surface during SEM observation.

EXPERIMENTAL RESULTS

Surface composition analysis

Secondary ion mass spectrometer (SIMS) was used to characterize the surface composition and depth profiles of elements in as-received aluminum foils.

Figure 2(a) and (b) shows the depth profiles of lead located on rolling lines and between rolling lines, respectively. Figure 2 shows clearly that for all locations, the concentration of lead in Foil A is much greater than that in Foil B. Figure 2 also shows that lead is enriched in the surface layers (to *ca.* 300–500 Å in depth) and approached null beneath the enriched layer. There is no difference in lead concentration for the two foils in the inner section.

Etched surface morphologies with HNO_3 pretreatment

To study further the differences of Foil A and Foil B, the two foils were degreased with 1 N NaOH, pretreated with 50% HNO_3 and then etched with direct current at 200 mA/cm^2 for different times. The etched surface morphologies for Foil A and Foil B are shown in Figs 3 and 4, respectively. The rolling line effect, i.e. the effect which results in concentrated etching along rolling lines leaving vast areas in between unattacked, are observed in both foils etched for 1 s (Figs 3(a) and 4(a)). After etching for 20 s, the rolling line effect is more serious in Foil A (Fig. 3(b)) than that in Foil B (Fig. 4(b)). It is observed that most of the etchings are on rolling lines for Foil A; in contrast, etchings are uniformly distributed both on rolling lines and in between rolling lines for Foil B.

The etch depth after 20 s was measured from the cross-sectional views of etched foils shown in Figs 5 and 6. The cross-section micrographs show clearly that surface etching, instead of tunnel etching, prevails on both foils.

In the literature, the effects of impurities in aluminum foil on the electrochemical etching process have been reported. It was found that the kind of impurities as well as their distributions have great influence on the etching behaviour. Other properties of the raw foil, such as grain size and cubicity, also have been mentioned. In the present work, the cubicity and grain size of the two foils were measured. The differences in grain size (180 μm for A, 200 μm for B) and cubicity (90.5% for A, 89.0% for B) are relatively small between the two foils, implying that they are not the major factors responsible for the surface morphology difference between the two etched foils.

In the preliminary work, the results of surface composition analysis by SIMS show that the most obvious difference between the two as-received foils is the concentration of element

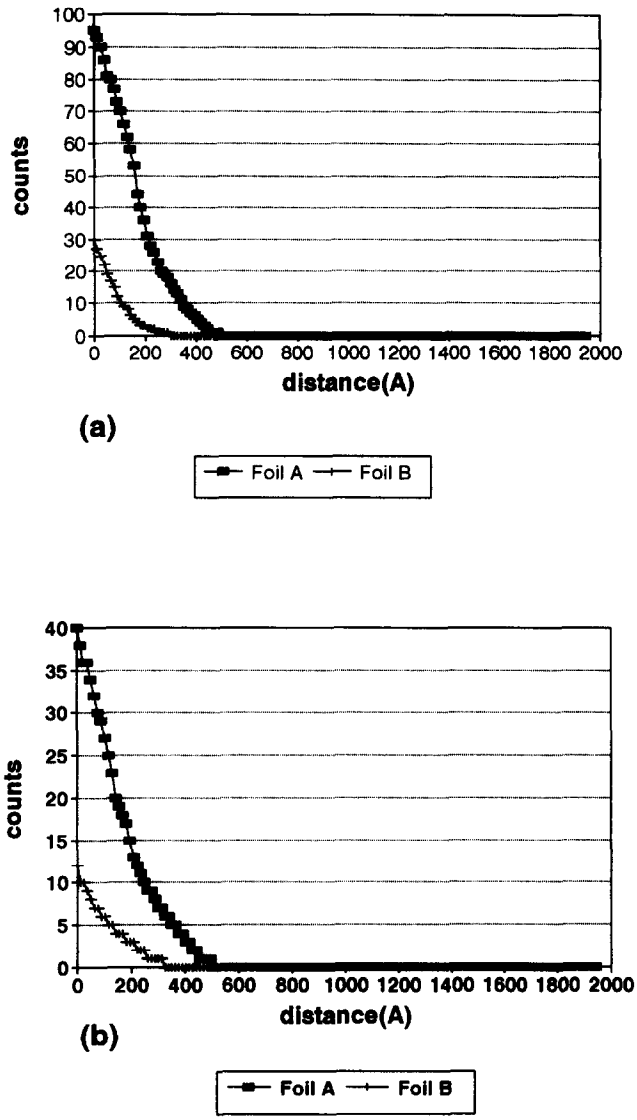

Fig. 2. The depth profiles of lead of two foils: (a) as-received, on the rolling line; (b) as-received, between the rolling line; (c) after $NaOH/HNO_3$ treatment, on the rolling line; (d) after $NaOH/HNO_3$ treatment, between the rolling line.

lead. Both aluminum and lead have the fcc crystal structure. However, their emf values and atomic sizes are quite different. It is possible that the difference in lead content and its distribution on the two foils results in different appearance of their etched surface morphologies.

Etched surface morphologies with $Pb(NO_3)_2$ pretreatment

To further understand the effect of lead on the electrochemical etching behaviour, lead was introduced intentionally onto the foil. The two foils were degreased with NaOH,

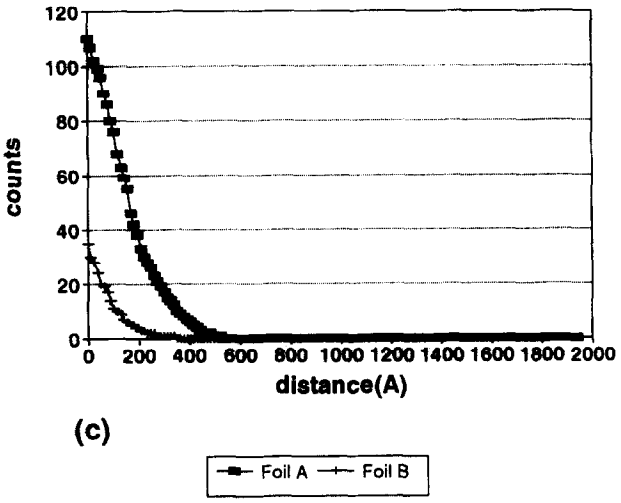

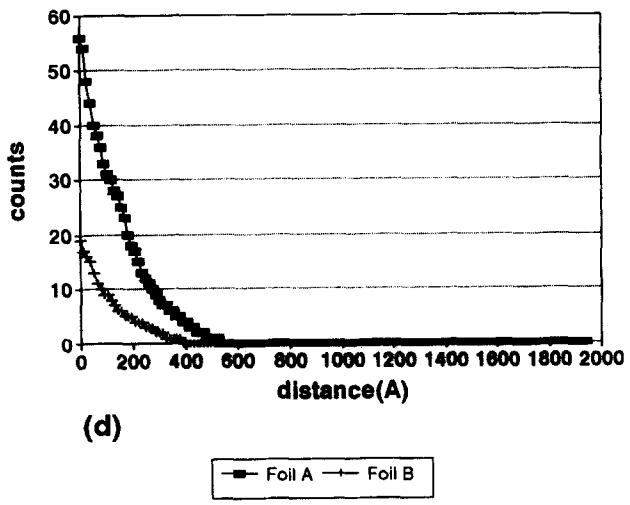

Fig. 2. (*Continued*)

pretreated with $Pb(NO_3)_2$ for 30 s and then DC-etched. The etched surface morphologies for both Foil A and Foil B are shown in Figs 7 and 8, and the corresponding cross-sectional views are shown in Figs 9 and 10, respectively.

It is clear from Fig. 7 that $Pb(NO_3)_2$ pretreatment changes tremendously the etching behavior of Foil A. The rolling line effect disappeared clearly and pits distributed uniformly over the foil surface. Cross-section micrography (Fig. 9) shows that most of the etched pits, or so called "tunnels", grew in perpendicular to the foil surface, and increased in length with etching time. The tunnel length is about 8 μm after etching for 1 s and increased to about 45 μm after etching for 20 s. In contrast, only very few and relatively short tunnels were observed for the same foil without $Pb(NO_3)_2$ pretreatment (Fig. 5).

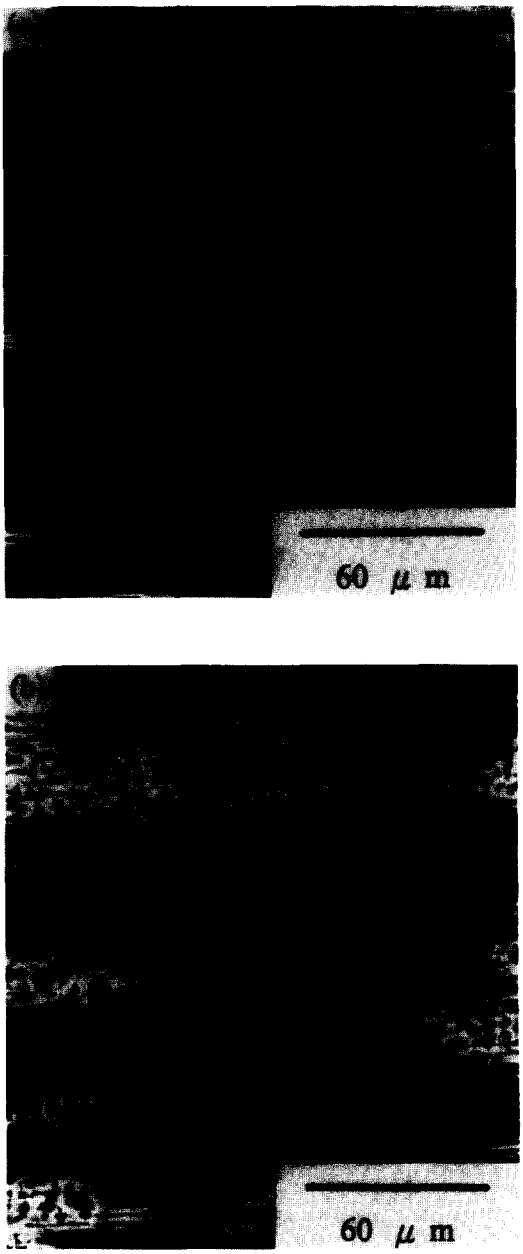

Fig. 3. Surface morphologies of HNO_3-pretreated Foil A after DC-etching for (a) 1 s, (b) 20 s.

It is interesting to find that $Pb(NO_3)_2$ pretreatment has no significant effect on the etching behaviour of Foil B. Etchings were mainly initiated along rolling lines and grew in parallel to the foil surface, i.e. surfacial etching rather than tunnelling (Fig. 8). No tunnel was observed even after DC-etching for 20 s, Fig. 10.

From the above results, it appears that the $Pb(NO_3)_2$ pretreatment is capable of

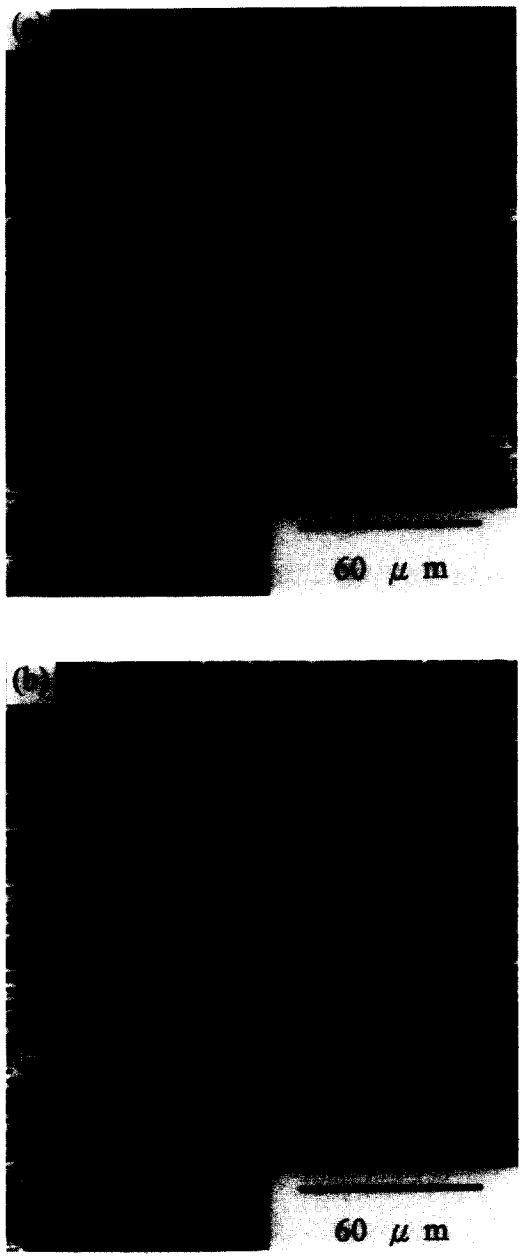

Fig. 4. Surface morphologies of HNO_3-pretreated Foil B after DC-etching for (a) 1 s, (b) 20 s.

modifying the two foil surfaces somehow in different ways. Therefore, it entails examining the $Pb(NO_3)_2$-treated foil surfaces before the resulting difference in etching behaviour can be explained.

Mapping of lead

It is possible that immersion of Al foil in $Pb(NO_3)_2$ may result in the plating out of

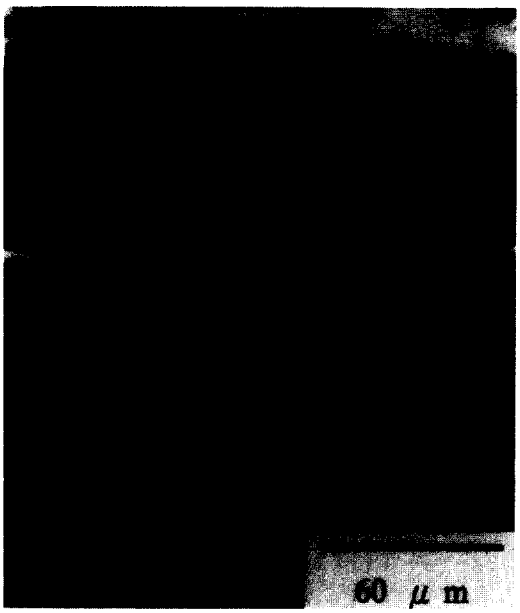

Fig. 5. Cross-sectional view of HNO_3-pretreated Foil A after DC-etching for 20 s.

metallic Pb on the foil surface, due to the difference in standard redox potentials of the two elements. For further understanding the difference of etched surface morphologies in the two foils with $Pb(NO_3)_2$ pretreatment, the surface composition was revealed by backscattering electron image (BEI) mode of SEM examination allied with EDS analysis.

Figure 11 shows the results of BEI morphology. The white spots on both foils (Fig. 11(a)

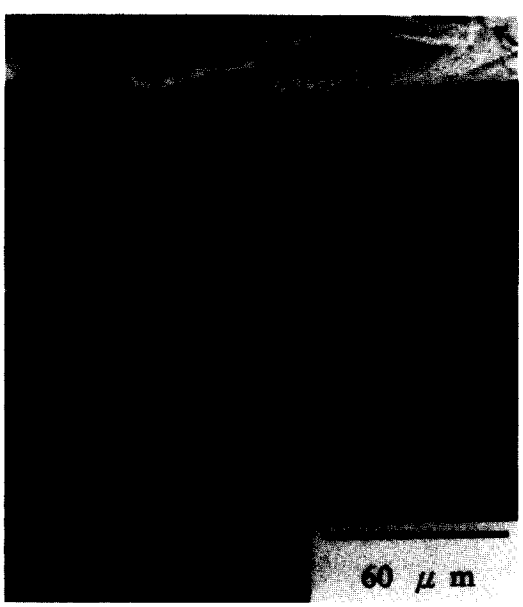

Fig. 6. Cross-sectional view of HNO_3-pretreated Foil B after DC-etching for 20 s.

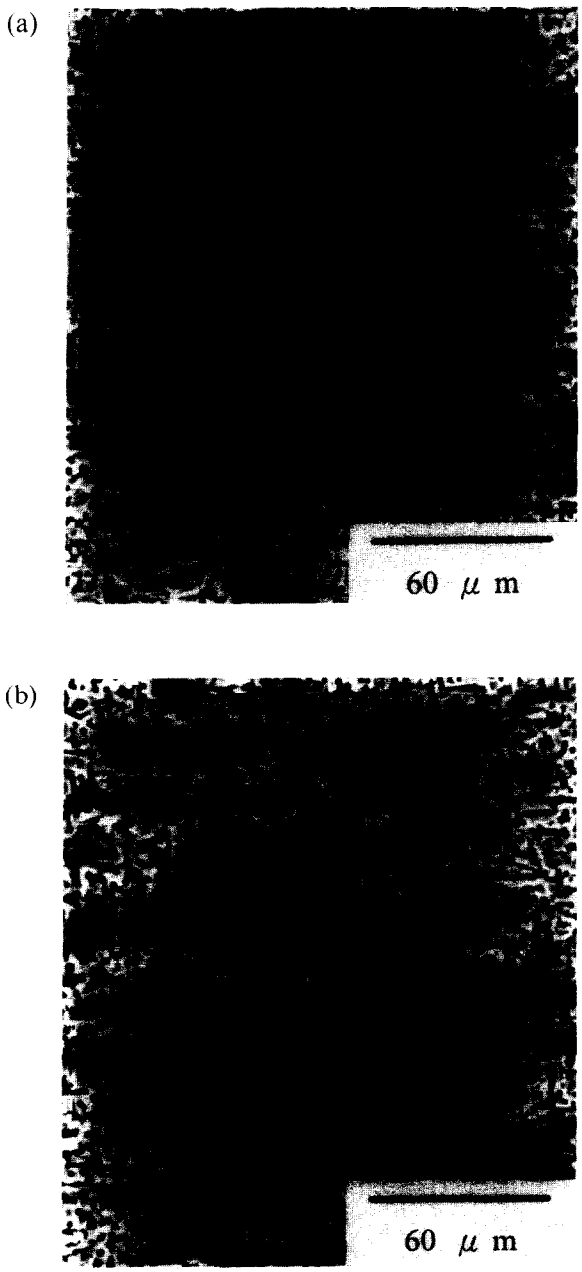

Fig. 7. Surface morphologies of Foil A pretreated in $Pb(NO_3)_2$ for 30 s, DC-etched for (a) 1 s, (b) 20 s.

and (b)) were further identified with EDS analyses. Figure 11(c) and (d) shows that the major components of the white spots are lead and aluminum. The observed lead is most possibly a resultant of the immersion–reduction reaction which occurred during the $Pb(NO_3)_2$ pretreatment.

Comparing Fig. 11(a) with (b), the white spots on Foil A assume an apparently larger

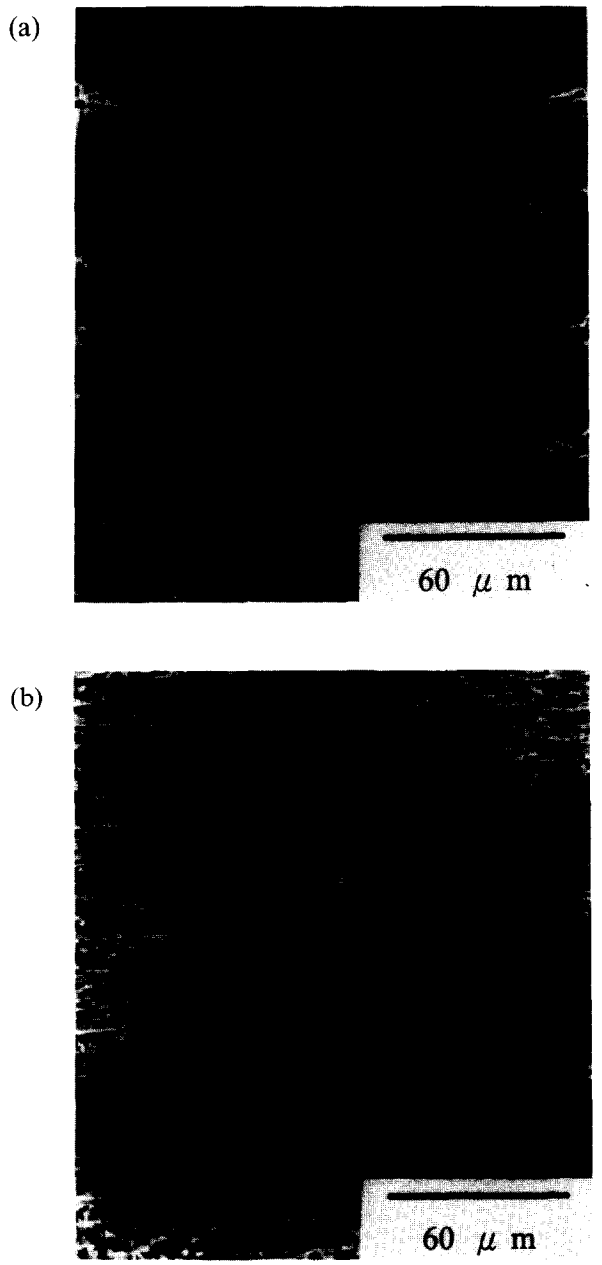

Fig. 8. Surface morphologies of Foil B, pretreated in $Pb(NO_3)_2$ for 30 s, DC-etched for (a) 1 s, (b) 20 s.

amount and a more uniform distribution feature than those on Foil B. Furthermore, most of the white spots on Foil B distributed along rolling lines. For as-received foils, SIMS depth profiles (Fig. 2) have shown that the concentration of lead in Foil A is much greater than that in Foil B, both on rolling lines and in between rolling lines. The points where as-received lead present may serve as preferential sites for lead deposition during $Pb(NO_3)_2$

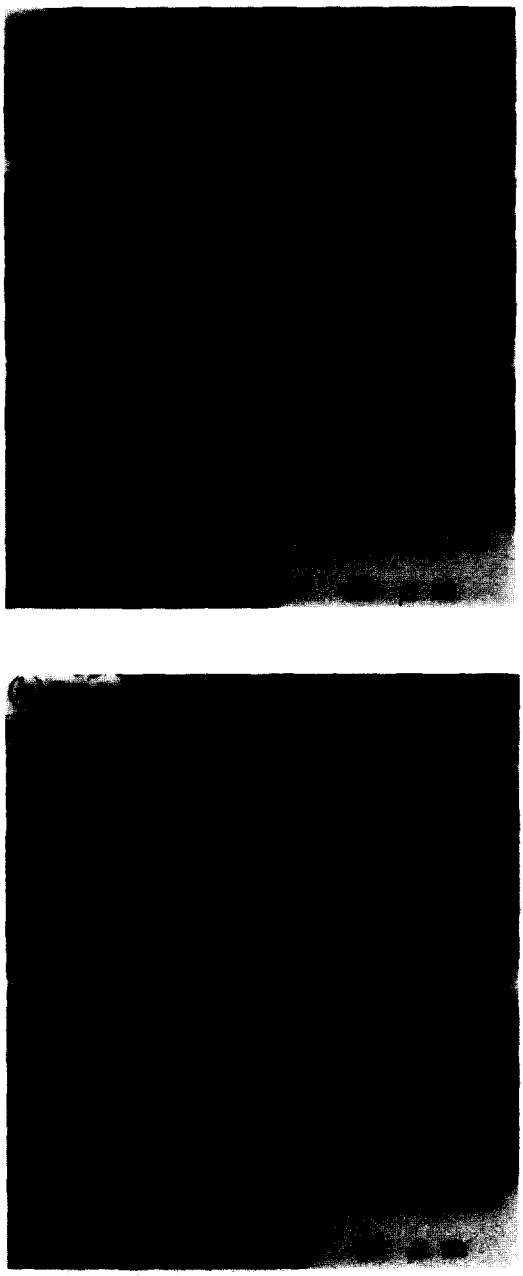

Fig. 9. Cross-sectional view of Foil A, pretreated in $Pb(NO_3)_2$ for 30 s, DC-etched for (a) 1 s, (b) 20 s.

pretreatment. Accordingly, one may conclude that, during the immersion–reduction reaction, Foil A has more uniform sites for lead deposition than Foil B. The differences in deposited lead concentration and distribution result in different etching morphologies of the two foils.

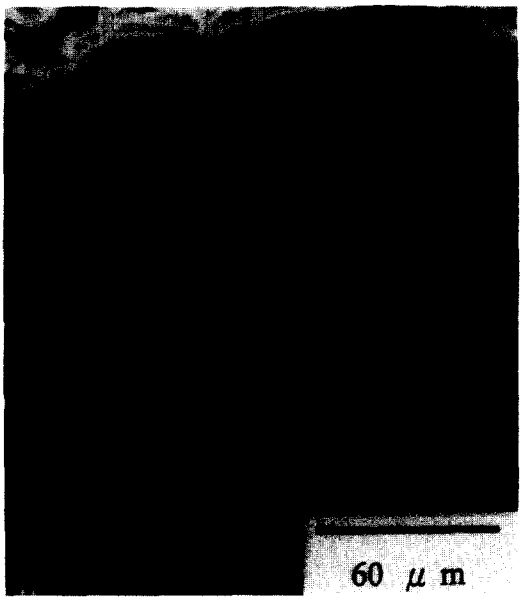

Fig. 10. Cross-sectional view of Foil B, pretreated in $Pb(NO_3)_2$ for 30 s, DC-etched for 20 s.

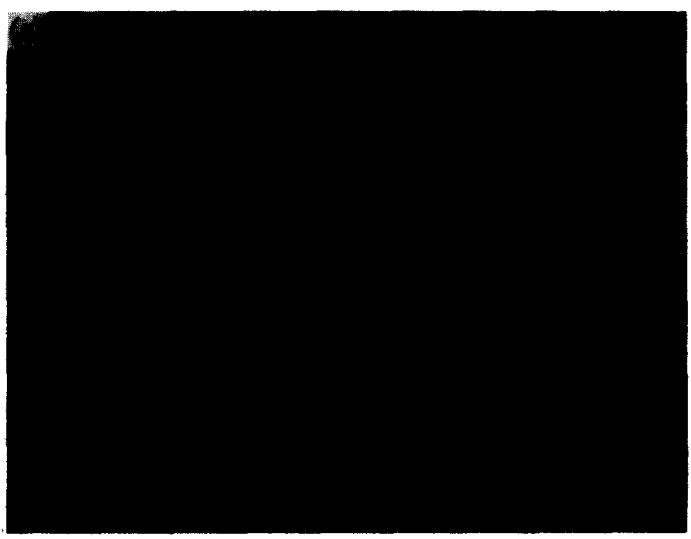

Fig. 11. BEI mode SEM micrographs of the two foils after pretreating in $Pb(NO_3)_2$ for 30 s: (a) Foil A; (b) Foil B. The white spots in the Al matrix are deposited lead as identified by EDS analyses shown in (c) Foil A and (d) Foil B.

Pitting potential

The pitting potentials for Foil A and Foil B with HNO_3 pretreatment are found to be -0.98 and -1.0 V, respectively. The effect of $Pb(NO_3)_2$ treatment on pitting potentials of the two foils was also studied. For Foil A, which has higher as-received lead content, the introduction of lead into the pretreatment solution results in a slight shift of pitting potential

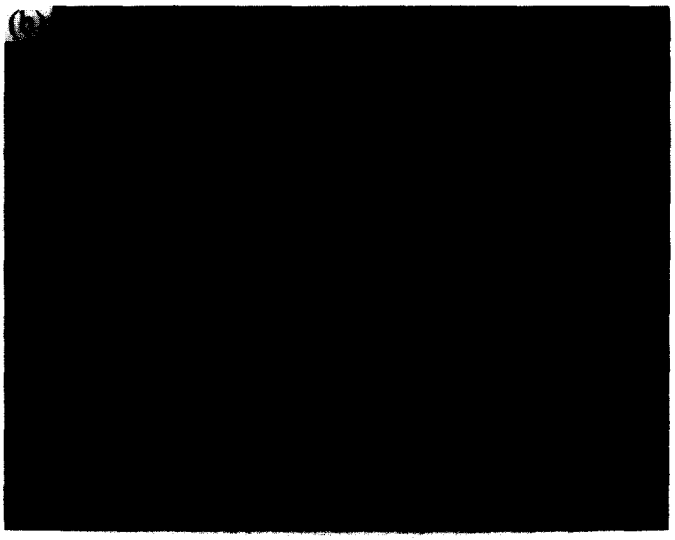

Fig. 11. (*Continued*)

from -0.98 to -1.02 V. The pitting potential for Foil B, with lower as-received lead content, shifts toward a more active value from -1.0 to -1.15 V.

DISCUSSION

The above studies show that for both types of foil with HNO_3 pretreatment most of the etchings are created along rolling lines. Rolling lines are a high strain area. Much research has indicated that there is a high concentration of impurities distributed along rolling lines. In this work, SIMS measurements show that the lead impurity is also concentrated in rolling lines (Fig. 2). From the metallurgical point of view, it is not difficult to understand that the aluminum lattice will be distorted no matter how impurities exist in aluminum (interstitial or substitutional); this will make a higher local lattice energy through the contribution of the strain energy. It is believed that there are high concentrations of impurities and dislocations located in rolling lines which serve as the major sites for pit initiation.

The rolling line effect is related partly to the content of lead in foils. For example, Foil A, which has a higher lead content, has a stronger rolling line effect than Foil B. For HNO_3 pretreated foils, it is observed that the rolling line effect still occurs on Foil A after etching for 20 s, whereas the rolling line effect does not occur so apparently for Foil B. This is because the potential of lead is much higher than that of aluminum; during the electrochemical etching process, lead acts as a cathode and aluminum as an anode. Lead and aluminum form a local cell. The etchings initiate at the sites where the larger local cell exists, i.e. along the rolling line, which provides a larger driving force. For the foil with lower lead content, etchings start along rolling lines and then spread over between rolling lines as etching time increases. On the other hand, foil with higher lead content would possibly produce more local cells along rolling lines. Consequently, etchings are mainly located along the rolling lines. Concerning the above reasoning, one may argue that lead contained in the bulk metal could be dissolved once and then redeposited, and thus the surface and in-depth distributions of lead could be varied after $NaOH/HNO_3$ treatment. The argument is

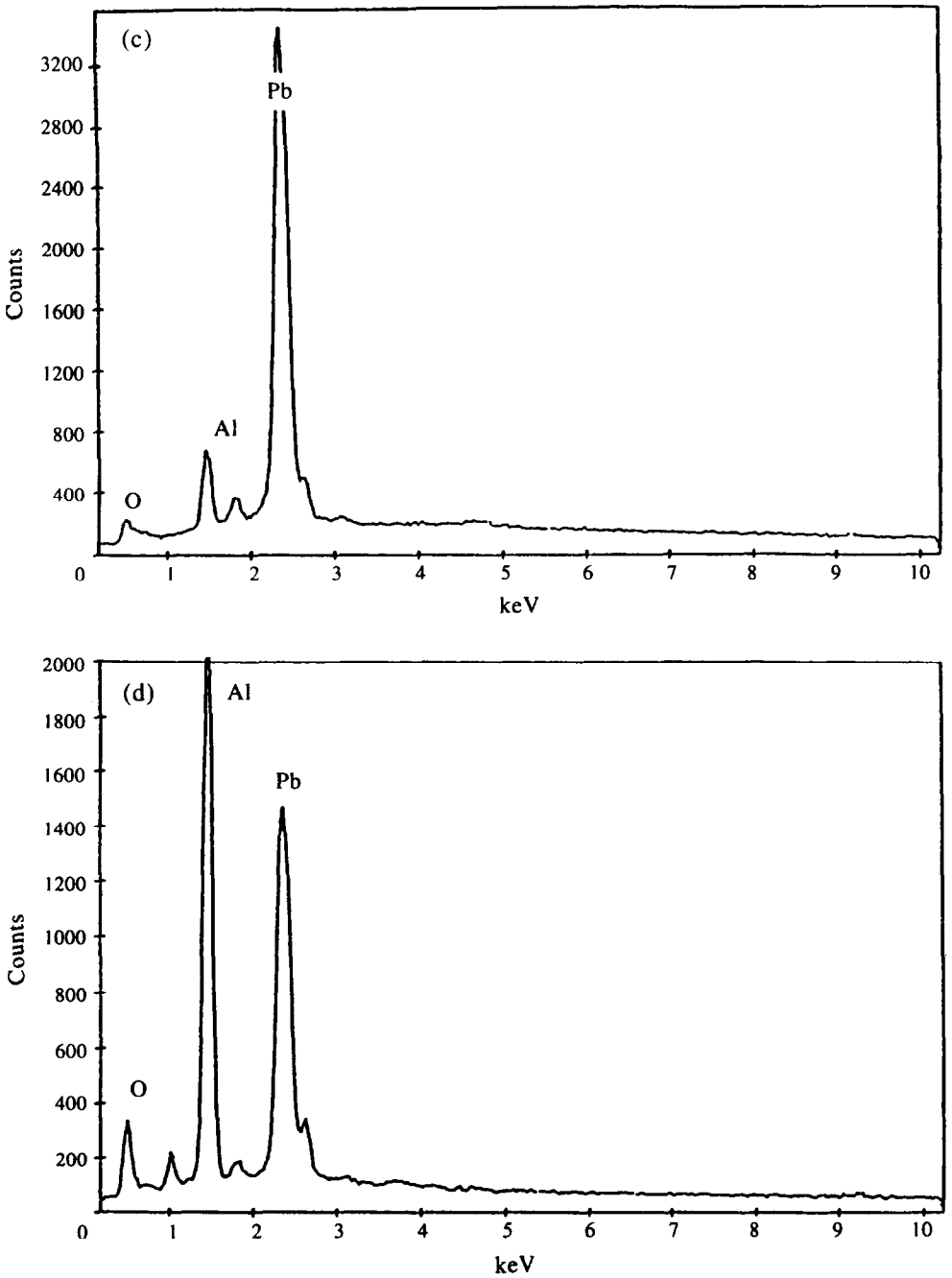

Fig. 11. (*Continued*)

clarified in Fig. 2(c) and (d), which shows the surface and in depth distributions along and between rolling lines are very similar to those of as-received foil (Fig. 2(a) and (b)). This concludes that the concentrations of lead in Foil A, both surface and in depth and both along and between rolling lines, are responsible dominantly for the more serious rolling line effect appeared in DC-etched Foil A after $NaOH/HNO_3$ treatment.

For the foil with the higher lead content, the rolling line effect can be improved to increase tunnel forming ability with the introduduction of $Pb(NO_3)_2$ pretreatment. As shown in Fig. 7, the etching pits on Foil A are distributed uniformly over the entire surface for an etching time as short as 1 s. The corresponding cross-sectional view in Fig. 9(a) clearly shows that most of the etchings were tunnel type. On the other hand, the improving ability of $Pb(NO_3)_2$ pretreatment is relatively small for foils with lower lead content. Figure 8 shows that the rolling line effect still exists for Foil B even after etching for 20 s. Figure 10 shows that most of the etchings are still parallel with the surface.

For raw foils with a higher concentration of lead, there are more lattice strain sites both in and in between the rolling lines. The activation energy for lead reduction is smaller during $Pb(NO_3)_2$ pretreatment. Consequently, higher concentrations of deposited lead can be obtained both in and inbetween rolling lines. This can be proved from lead composition mapping analysis (Fig. 11) which shows that deposited lead is distributed uniformly in Foil A. However, in Foil B, with lower as-received lead content, the deposited lead is present only within rolling lines.

The pitting potentials shift towards a more active direction as a consequence of lead reduction after immersing in $Pb(NO_3)_2$. The potential shift is due to formation of Al//Pb local cells. It should be noticed that the deposited lead is a second phase; it cannot be confused with the as-received lead in raw foils, which is in solid solution state in high purity (99.99%) aluminum.

The distribution of deposited lead would affect the extent of potential shift. For Foil B, which has a lower as-received lead content and non-uniform distribution of deposited lead, the Al//Pb local cells are heavily concentrated in rolling lines. The free energy in rolling line increases substantially due to strain energy resulting from incoherent interface between Al-matrix and deposited lead. Consequently, the pitting potential decreases significantly and pitting corrosion occurs along rolling lines. On the other hand, Foil A assumes a uniform distribution of deposited lead; this makes dispersed Al//Pb local cells and results in pits being created uniformly over whole foil surface. Since Al//Pb local cells are not localized in rolling lines, the pitting potential shifts only slightly toward active direction.

A further experiment, to support the viewpoint, was performed on Foil B. In the experiment, the immersion time of $Pb(NO_3)_2$ pretreatment was doubled, i.e. 60 s, before DC-etching. The etched surface morphologies are shown in Fig. 12, and cross-sectional views are shown in Fig. 13. It is apparent from Fig. 12 that the rolling line effect disappears totally after DC-etching for 1 s and tunnel-type etching dominates clearly in the process (Fig. 13). Obviously, the above results are derived from a higher concentration of lead, due to doubling the immersion time and being uniformly deposited on the foil surface.

CONCLUSIONS

In this work, the effects of lead impurity on the etched morphology of commercial grade high purity aluminum foils were investigated. The content of lead impurities in as-received foils as measured through SIMS depth profile was found to have a close relationship with

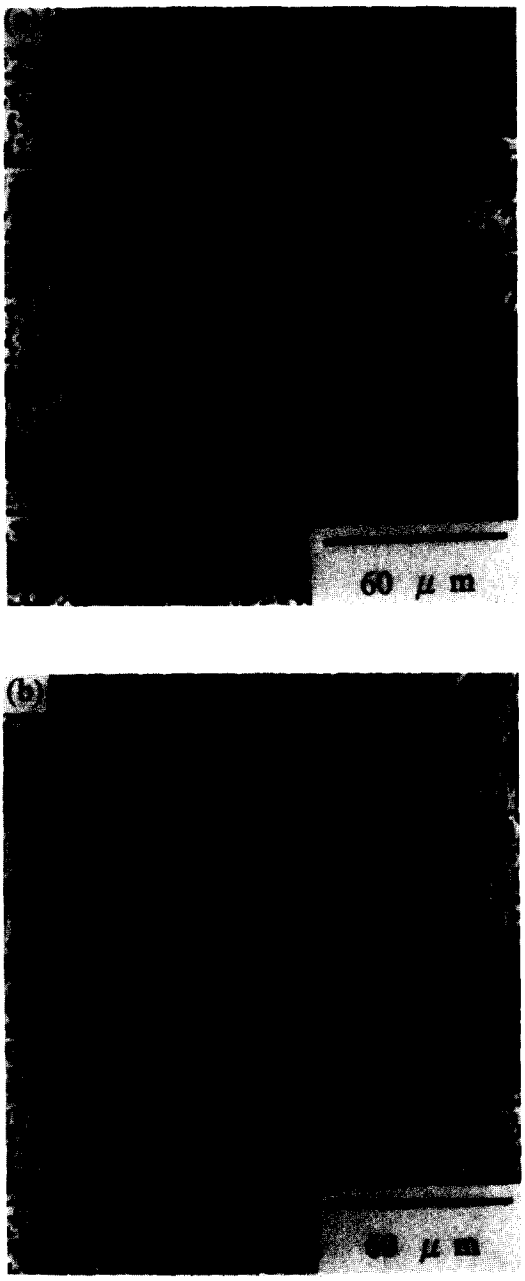

Fig. 12. Surface morphologies of Foil B pretreated in $Pb(NO_3)_2$ for 60 s, DC-etched for (a) 1 s, (b) 20 s.

the etched morphology. The foils with a higher as-received lead content present a more serious rolling line effect after DC-etching.

The rolling line effect can be improved or overcome through introducing deposited lead on a foil surface by immersion of the foil into $Pb(NO_3)_2$ solution prior to DC-etching. For the foils with a higher as-received lead content, it is reckoned and found that there were

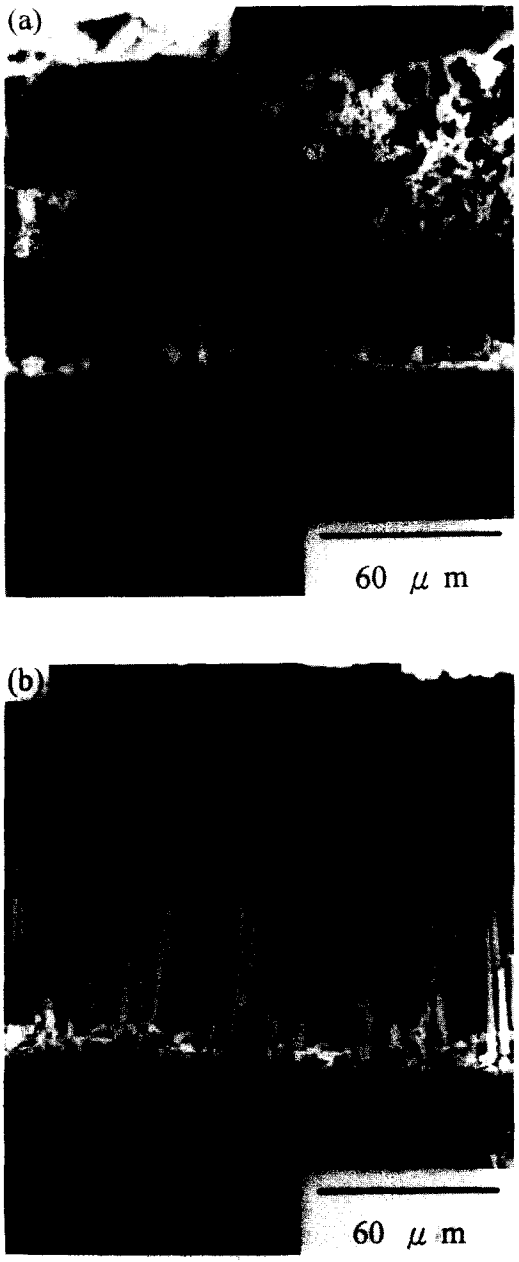

Fig. 13. Cross-sectional view of Foil B pretreated in $Pb(NO_3)_2$ for 60 s, DC-etched for (a) 1 s, (b) 20 s.

more sites for Pb nucleation; this results in higher concentrations of lead being uniformly deposited on the foil surface. The etched morphology therefore assumes a uniformly distributed tunnel structure.

For the foils with a lower as-received lead content, it is considered and found that most of the lead impurity is distributed preferentially in rolling lines: the deposited lead

consequently was also concentrated in this region. The high concentration of Al//Pb local cells in rolling lines greatly reduces the corrosion resistance of the foils. The pitting potential shifted 150 mV toward active direction. Since the Al//Pb local cells serve as primary sites for pitting corrosion, most of the etchings were distributed along rolling lines and grew parallel to the foil surface. Development of vertical tunnel etching was then inhibited.

REFERENCES

1. K. Arai and T. Suzuki, *Light Metal* **31**, 675 (1981).
2. R. Bakish, E. Z. Border and R. J. Kornhass, *J. electrochem. Soc.* **109**, 791 (1962).
3. R. Bakish, *Electrochem. Technol.* **6**, 192 (1968).
4. Z. Q. Zheng and W. B. Zhang, *J. China Inst. Central South Inst. Mining Metal* **1**, 111 (1983).
5. R. Bakish, R. J. Kornhass and E. Z. Border, *J. electrochem. Soc.* **1**, 358 (1963).
6. O. Seri, *Surface Tech.* **44**, 23 (1993).
7. R. B. Diegle, *J. electrochem. Soc.* **121**, 583 (1974).
8. G. Muriset, *Ibid.* **99**, 285 (1952).
9. L. V. Alphen, P. Nauwen and L. Slakhorst, *Z. Metallkd* **70**, 158 (1979).
10. G. E. Thompson and G. C. Wood, *Corros. Sci.* **8**, 721 (1978).
11. K. Arai, T. Suzuki and T. Atsumi, *J. electrochem. Soc.* **132**, 1667 (1985).
12. H. Biloni, M. F. Bolling and H. A. Domain, *TMS-AIME* **233**, 1926 (1965).
13. A. P. Bond, M. F. Bolling and H. A. Domain, *Tech. Rep. No. SL-65-50, Ford Motor Company Science Laboratory* (1965).
14. I. Nagata, *Aluminum Electrolytic Capacitor*, p. 186, Japan Chemical Condensor Corp. (1983).
15. K. Fukuoka and M. Kurahashi, *The Electrochemical Society of Japan conference*, Fukoka (1993).
16. W. Lin, G. C. Tu, C. F. Lin and Y. M. Peng, unpublished work.
17. C. G. Dunn, R. B. Bolon, A. S. Alwan and A. W. Stirling, *J. electrochem. Soc.* **118**, 381 (1971).